ELSEVIER

Ceramics International 29 (2003) 939–946

CERAMICS INTERNATIONAL

www.elsevier.com/locate/ceramint

Binder removal and microstructure with burnout conditions in $BaTiO_3$ based Ni-MLCCs

Ungyu Paik[a,*], Kyung-Moo Kang[b], Yeon-Gil Jung[b], Jonghee Kim[c]

[a]*Department of Ceramic Engineering, Hanyang University, Seoul 133-791, South Korea*
[b]*Department of Ceramic Science and Engineering, Changwon National University, Changwon, Kyungnam 641-773, South Korea*
[c]*Samsung Electro-mechanics Co., Ltd., Suwon, Kyunggi-do 442-773, South Korea*

Received 13 May 2002; received in revised form 17 January 2003; accepted 31 January 2003

Abstract

The burnout conditions in multilayer ceramic capacitors (MLCCs) have been investigated to optimize the binder removal condition and to control the microstructure during the burnout process. MLCCs showed a delamination for the heating rate of 7 °C/min at 200 °C, and 6 °C/min at 250 °C and 300 °C in the ambient atmosphere. The heating rate affected the pore size distribution and mean pore size, showing the smaller and larger mean pore size in the reducing and at higher temperature, respectively. The cumulative pore surface area was dependent on the burnout temperature rather than the heating rate. The minimum pore surface area could be obtained at 300 °C with the heating rate of 3 °C/min, in which the pores were connected to be an open structure. The atmosphere and temperature affected the burnout microstructure related to the binder removal without the effect of the heating rate.

Keywords: B. Microstructure; B. Porosity; D. $BaTiO_3$; E. Capacitors; Binder burnout

1. Introduction

In the fabrication process of multilayer ceramic capacitors (MLCCs), the burnout process to remove binders used for casting is one of the key processing steps. When the sufficient control in the binder burnout process is not achieved, the electrode (particularly, base metal electrode, e.g. Ni, which has recently replaced the Ag–Pd alloys for the production cost [1]) can be partially oxidized, resulting in the fatal defects in the firing process. Therefore, to prevent the oxidation, the burnout process has been performed in a protective atmosphere using N_2 and Ar [2–7]. Atmosphere must be also controlled at the following stages of the heat-treatment process, including the sintering and post-annealing processes.

For high capacitance in MLCCs, reducing of the active thickness is a much more effective strategy for increasing volume efficiency than increasing of dielectric constant alone. For this purpose, smaller size powders as the dielectric material and internal electrode need to be used, which has to give more attention to the burnout process for preventing the oxidation of the electrode and for controlling the residual carbon from the incomplete binder removal in the burnout process [8–11]. Also, a pore structure formed by the binder removal and a relationship between microstructure and burnout condition are important for the reliability and mechanical property of MLCCs.

There are many reports on the relationships between microstructure and dielectric properties, including the sintering behavior of doped and undoped $BaTiO_3$ materials [2–5,12]. And limited literature resources are available on the effect of sintering atmosphere on dielectric properties [10,11]. However, the effects of burnout conditions on the binder removal and microstructure in $BaTiO_3$ based Ni-MLCCs specified X7R dielectric characteristic, have not been shown in the literature.

The present work describes the influences of atmosphere, temperature, and heating rate on the binder removal and microstructure in $BaTiO_3$ based Ni-

* Corresponding author. Tel.: +82-2-2290-0502; fax: +82-2-2281-0502.
E-mail address: upaik@hanyang.ac.kr (U. Paik).

0272-8842/03/$30.00
doi:10.1016/S0272-8842(03)00049-X

MLCCs. The green MLCCs were fired under different conditions as functions of atmosphere, temperature, and heating rate. The relationships among burnout conditions, pore size distribution, cumulative pore surface area, hysteresis, and microstructure have been extensively investigated as well.

2. Experimental procedure

2.1. Sample preparation

$BaTiO_3$ (BT-04B, Sakai Co., Japan) and Ni powders were used as the dielectric material and internal electrode, respectively. The dielectric formulation showing X7R characteristic was prepared by doping various metal oxide additives (Y_2O_3, $MgCO_3$, MnO_2, V_2O_5, Cr_2O_3) and glass frit (Ba–Ca–Si system), totaling less than 4 wt.% of the formulation.

The green MLCCs were prepared by the following procedure. The powder, organic binder (PVB series), dispersant, and plasticizer were mixed and dispersed in a nonaqueous media (mixture of toluene and ethanol). The green sheet with the thickness of ≈4 μm was prepared by the so-called slot-die method (on-roll method). After the electrode was printed on the green sheet, this was then laminated and isotropically pressed, then cut to green chips. The final dimensions of the green MLCCs after cutting were ≈4×2×2 mm with 330 actives.

2.2. Characterization

Thermal behavior of the chips was analyzed by thermogravimetric analysis (TG/DTA, SDT2960, TA Instrument, USA) in the ambient and argon atmospheres. The burnout atmosphere was chosen as the ambient and reducing atmospheres controlling H_2, Ar, O_2 and H_2O. The temperature and heating rate were selected as 200, 250 and 300 °C, and controlled as 1 °C/min to 7 °C/min with 1 °C interval, respectively, keeping the holding time of 1 h at each temperature.

An optical microscope (EPIPHON, Nikon, Japan) was used for the investigation of the entire condition in MLCCs after the burnout process. Pore size and distribution in MLCCs after the burnout process was

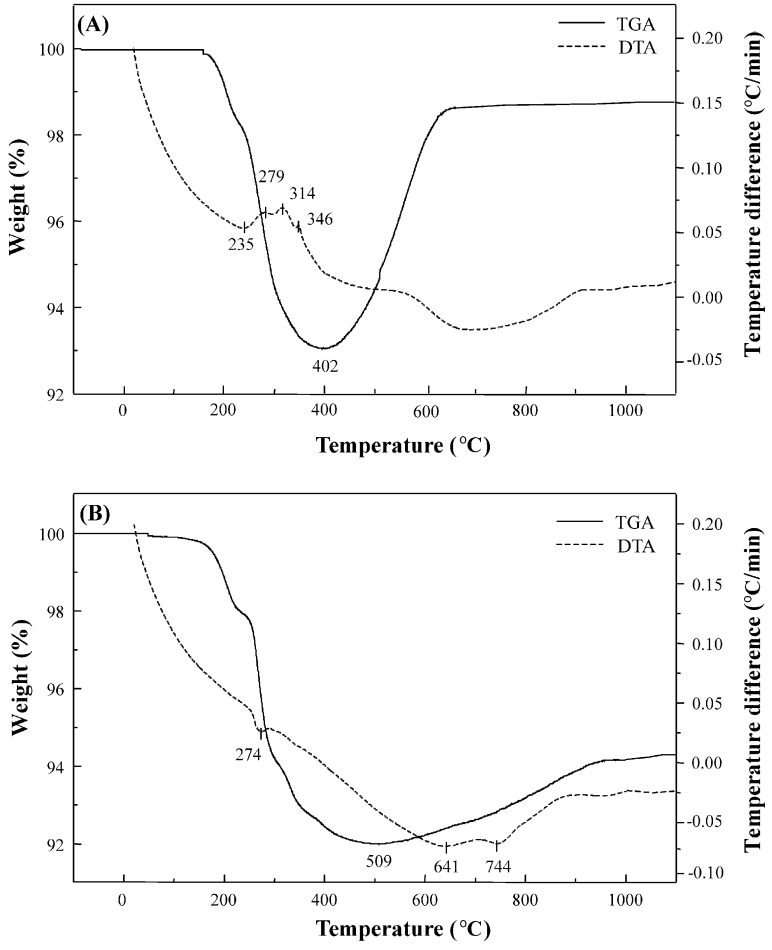

Fig. 1. TGA/DTA curves showing weight loss and gain of MLCCs after burnout process in (A) ambient and (B) argon atmospheres.

measured by a porosimetry (Autoscan-25, 60, Quantachrome Corp., Syosset, NY, USA), from which the cumulative pore surface area in MLCCs was compared and the pore structure was evaluated. Microstructure in fracture surface was observed by a scanning electron microscope (SEM, S2700, Hitachi, Japan).

3. Results and discussion

The burnout temperature to remove the organics added could be selected as 200, 250, and 300 °C based on the result of thermal analysis as shown in Fig. 1. Also, the information about the oxidation of the electrode could be obtained with the weight gain. In the ambient, the sudden weight loss was observed from ≈200 to ≈400 °C, and then the gain was detected to ≈660 °C, considered as the removal of the organics and the oxidation of the electrode, respectively.

The first peak at 235 °C is ascribed to the solvent and plasticizer evaporations, and the exothermic peaks at 279, 314, and 346 °C are believed to be due to the decomposition of the binder (PVB) [13]. The electrode was oxidized from ≈400 °C and fully oxidized at ≈660 °C in the ambient. However, a sudden weight change after ≈400 °C was not observed in the argon compared to the ambient, showing the weight loss to ≈500 °C and then a moderate increase. The weight gain in the argon can be considered as the oxidation of the electrode due to the reaction between the activated electrode and the oxygen vaporized and/or decomposed from the organics during the heat-treatment.

MLCCs displayed a delamination after the burnout process in the ambient condition as shown in Fig. 2. The delamination took place in the middle of MLCC from the heating rate of 7 °C/min at 200 °C and 6 °C/min at 250 and 300 °C, showing no delamination below these conditions. On the other hand, MLCCs prepared under the reducing condition ($Ar/H_2 = 97/3$) did not show defects such as the delamination and cracks with the naked eye at the heating rate of 6 °C/min and 7 °C/min in the ambient condition even if these are not shown as photograph. This result indicates that it is necessary to burnout at slower heating rate in order to prevent the delamination in the burnout process of MLCCs. Slow heating rate, in particular, is indispensable to the desired burnout in the ambient condition.

In addition, the delamination was created at the interface between the dielectric and electrode layers (even the result is not shown in this paper) and at the

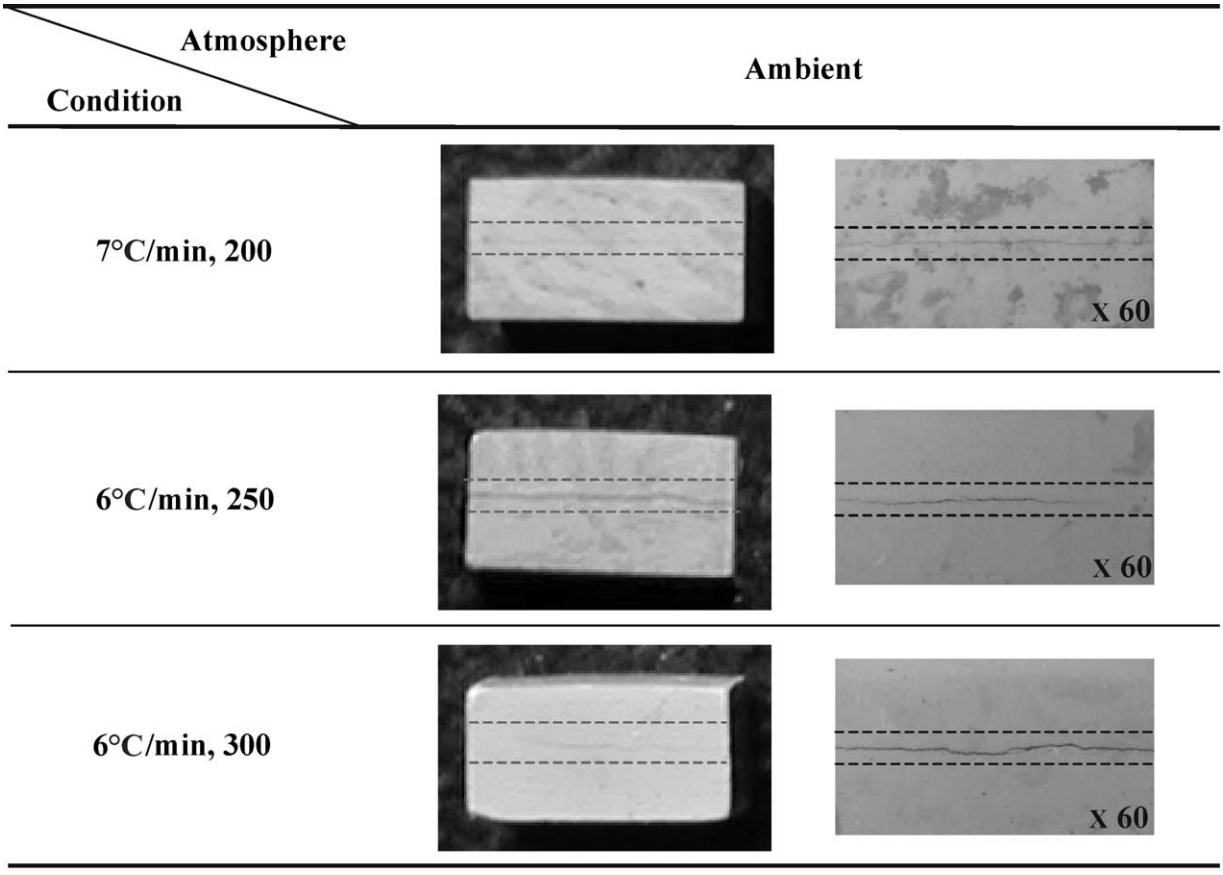

Fig. 2. Conditions of MLCCs after burnout process in ambient atmosphere as functions of heating rate and temperature.

middle of MLCCs. The cause can be considered as following: (1) insufficient pressing in laminating process, (2) sudden oxidation of the electrode, and (3) combustion of the binder. Even though MLCCs prepared in the reducing condition did not show the delamination on the surface, MLCCs with faster heating rate is likely to include some inhomogeneous nature of particle compact. This results directly in the firing defects, for example, inner cracks and residual stresses, etc., taking disadvantages in the firing process. The effects of heating rate and temperature in the burnout process on the microstructure and residual stresses developed in the end products (MLCCs) are underway and will be reported later.

Fig. 3 shows the pore size distribution after the burnout process at 250 °C with different heating rate in the reducing condition. The pore size distribution was affected by the heating rate, showing the multi-modal distribution. The mean pore size increased from 0.075 to 0.02 μm with an increase of the heating rate from 1 to 5 °C/min, showing that the results of the pore size (even the result is not shown in this paper) were dependent on the atmosphere and temperature with the smaller and larger mean pore size in the reducing and at higher temperature, respectively.

Fig. 4 gives the cumulative pore surface area on the pore size associated with the binder removal during the burnout process in the reducing condition. The cumulative pore surface area was suddenly decreased at 300 °C (Fig. 4C). In a comparison among the amplitudes of cumulative pore surface area, the specimen had much smaller value as the higher burnout temperature. The cumulative pore surface area demonstrated inconsistent trend with a change of heating rate at each temperature. It was found that the cumulative pore surface area was dependent on the temperature rather than the heating rate and the full pore channel was not created until 250 °C. The appropriate burnout condition can be considered as the temperature of 300 °C and the heating rate of 3 °C/min, even though a relatively larger pore contributed to the cumulative pore surface area at 300 °C. On the other hand, the other factors in the burnout process, such as the pore structure and burnout microstructure, have to be considered.

More specifically, the form of pore channel (pore structure or pore shape) can be assumed with the hysteresis of intrusion and extrusion behaviors in a mercury porosimetry. Fig. 5 shows the comparison between intrusion and extrusion behaviors in MLCCs as a function of the heating rate at 250 °C in the reducing condition. The hysteresis behavior was very similar to each other except the heating rate of 5 °C/min, even though the absolute amounts of the intrusion and extrusion were different. In the cases of the burnout process at 250 °C with 1 °C/min and 3 °C/min (Fig. 5A and B), 80–90% of the total mercury intruded remained in MLCCs. It is evident that the pore shape is a so-called ink-bottle pore with a narrow neck and a large volume, explained by the assumption of cylindrical pores in a mercury porosimetry [14,15]. In the other hysteresis (Fig. 5C), the extrusion curve completely overlapped the intrusion curve, indicating that the pore shape is the ink-bottle pore with a broad neck. However, it can be argued that pore shape and structure will be determined by the mercury intrusion/extrusion behaviors (hysteresis behavior), because the amount of mercury retained by the sample will be influenced by a combination of at

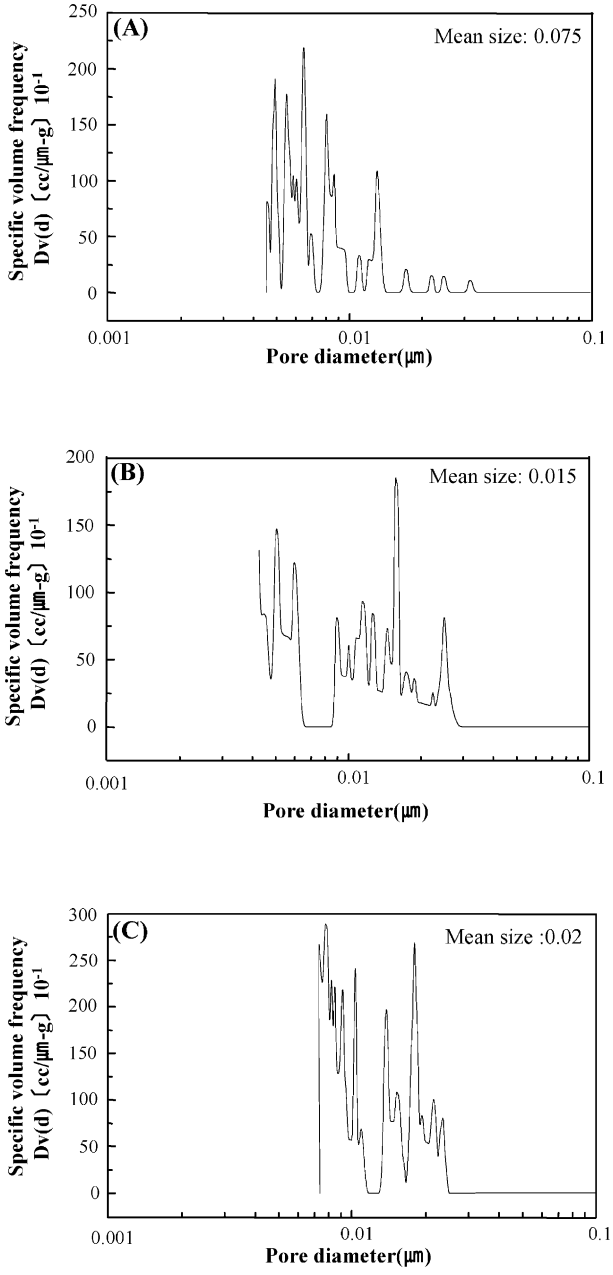

Fig. 3. Pore size and distributions of MLCCs after burnout process at 250 °C as a function of heating rate in reducing atmosphere: (A) 1 °C/min, (B) 3 °C/min, and (C) 5 °C/min.

least two factors: the shape of the pores and the value of the contact angle [16].

Many reports have been offered to account for the experimental observation that mercury extrusion curves do not overlap intrusion curves [15–20]. Three explanations appear to be favored by different groups in the literature: (1) the ink-bottle pore assumption [14–16], (2) network effects [17,18], and (3) a pore potential theory [19]. Usually, the pores of different size are assumed to be all of the same regular shape (e.g. cylinders or slits) and generally each pore is assumed to behave independently. In our study, the volume of mercury intruded was increased with an increase of the heating rate and the first pressure for intrusion was delayed with a decrease of the heating rate. These results are well consistent with the observation of the pore size distribution (Fig. 3) and cumulative pore surface area (Fig. 4B). Therefore, the specimen burned-out process at a slower heating rate will show the pore structure of narrower necks and larger inner volume than that at a faster

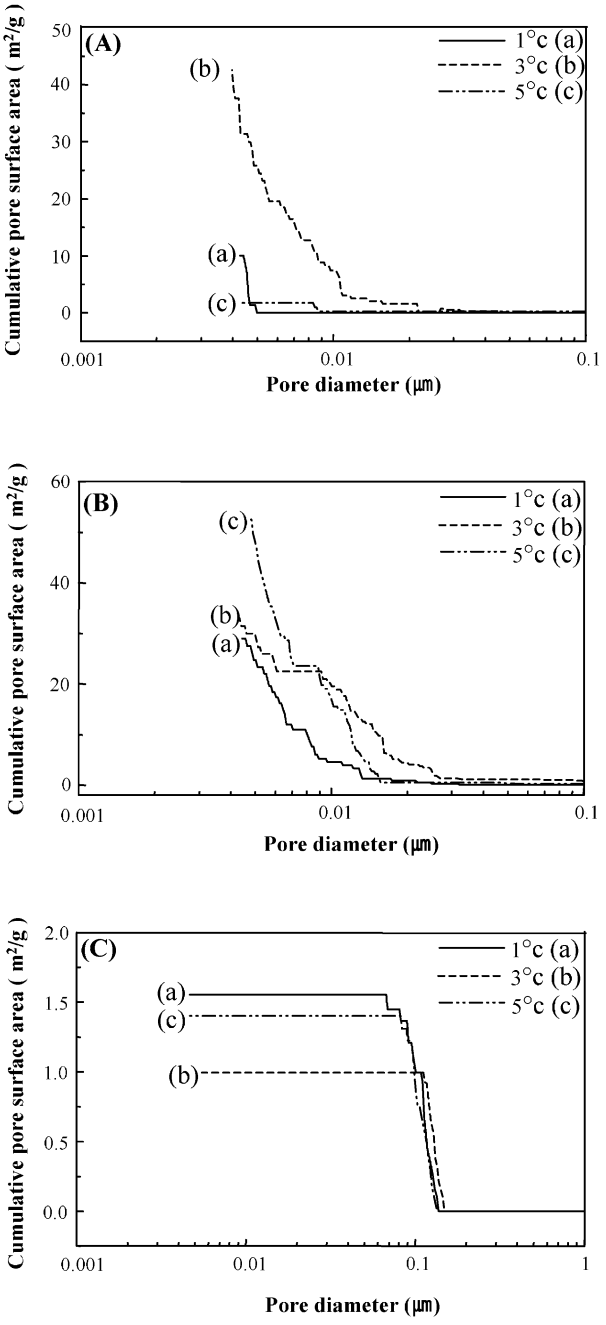

Fig. 4. Cumulative pore surface area as functions of heating rate and temperature in reducing atmosphere: (A) 200 °C with (a) 1 °C/min, (b) 3 °C/min, (c) 5 °C/min; (B) 250 °C with (a) 1 °C/min, (b) 3 °C/min, (c) 5 °C/min; (C) 300 °C with (a) 1 °C/min, (b) 3 °C/min, (c) 5 °C/min.

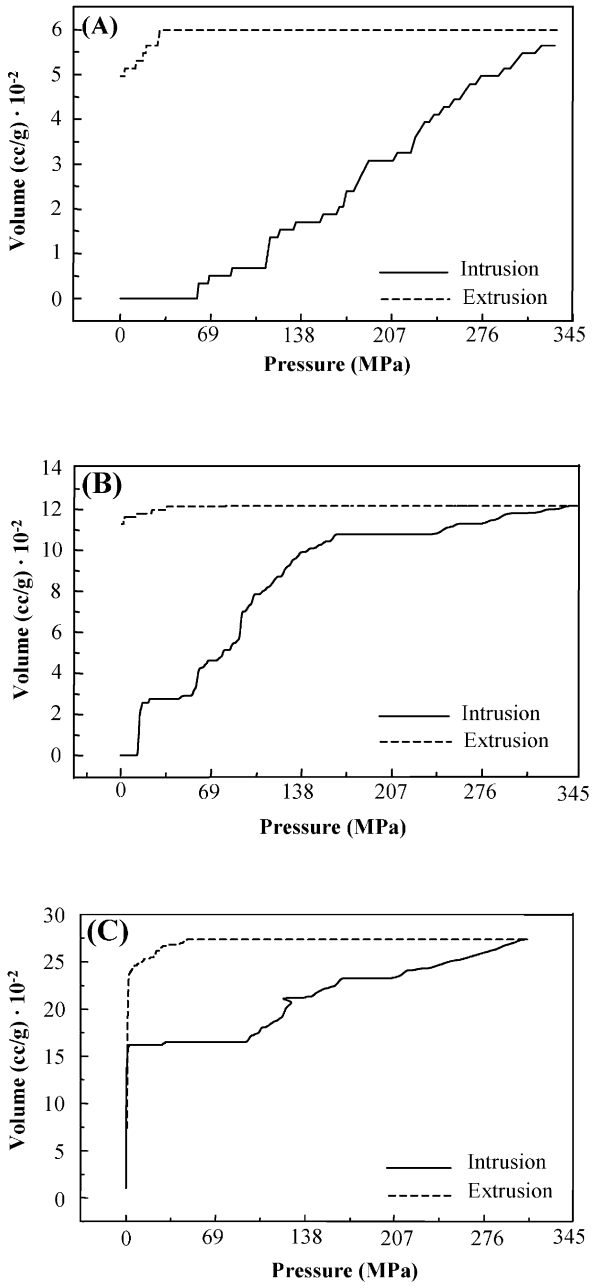

Fig. 5. Intrusion and extrusion curves of MLCCs after burnout process at 250 °C as a function of heating rate in reducing atmosphere: (A) 1 °C/min, (B) 3 °C/min, and (C) 5 °C/min.

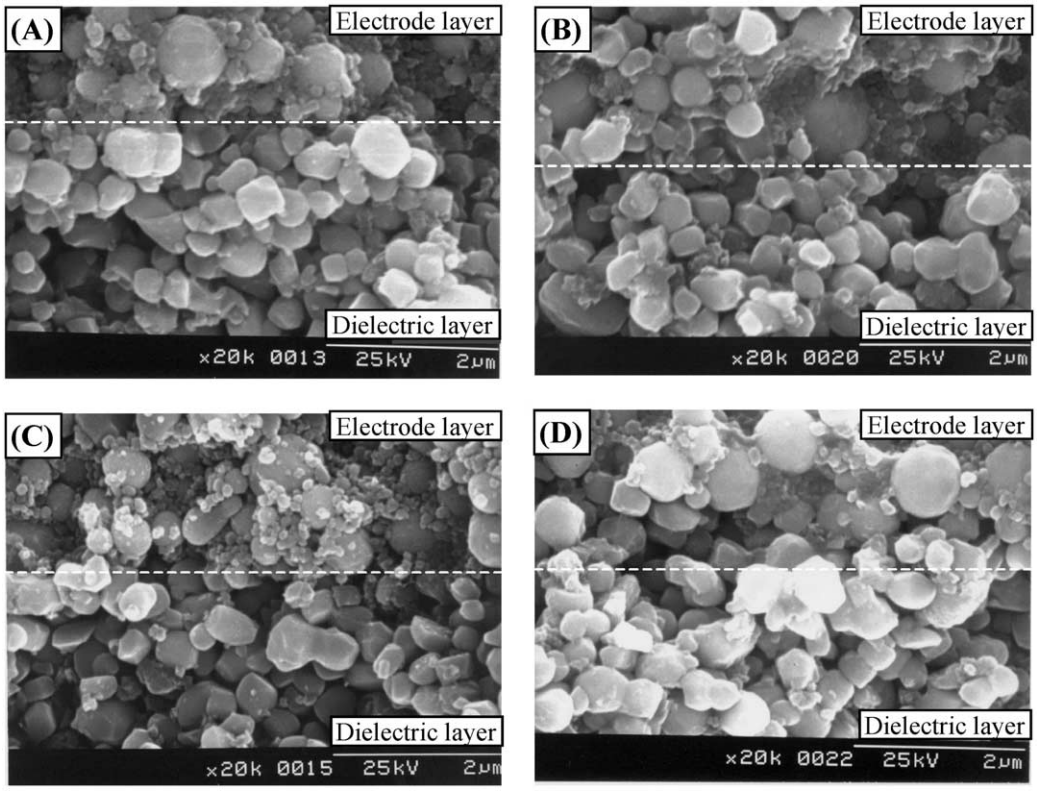

Fig. 6. Fracture surface of MLCCs after burnout process at 250 °C in the ambient and reducing atmospheres: (A) 3 °C/min in ambient atmosphere, (B) 3 °C/min in reducing atmosphere, (C) 5 °C/min in ambient atmosphere, and (D) 5 °C/min in reducing atmosphere.

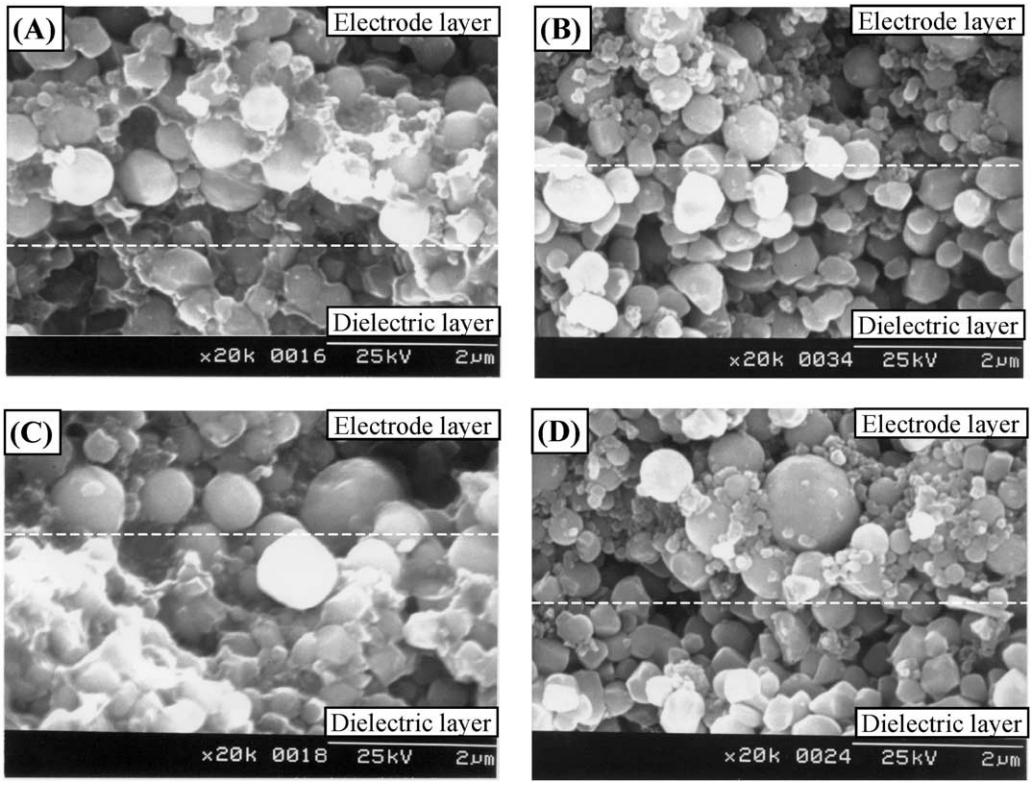

Fig. 7. Fracture surface of MLCCs after burnout process in reducing atmosphere: (A) 200 °C with 3 °C/min, (B) 300 °C with 3 °C/min, (C) 200 °C with 5 °C/min, and (D) 300 °C with 5 °C/min.

heating rate, indicating that faster heating rate is preferred for the better burnout condition in the reducing condition.

The effects of atmosphere, heating rate, and temperature on the microstructure related to the binder removal can be more clearly observed from the SEM images in fracture surface (Figs. 6 and 7). The ambient condition (Fig. 6A and C) was more effective in removing the binder than the reducing one (Fig. 6B and D). It remained lots of binder between particles after the burnout process in the reducing condition, whereas, in the ambient condition, the particle surface was clearer as the evidence of the complete binder removal. However, the effect of the heating rate on the microstructure was not observed in either atmosphere. When the burnout process was performed in the reducing condition, the microstructure at 300 °C (Fig. 7B and D) was very similar to that at 250 °C in the ambient one (Fig. 6A and C). It was found that the atmosphere and temperature significantly affected the burnout microstructure related to the binder removal.

Based on the above results, it can be proposed in the optimization of burnout condition that the burnout process at higher temperature with faster heating rate must be performed in the reducing condition or that at lower temperature with slower heating rate in the ambient one. However, if the burnout process is performed with a faster heating rate even in the reducing condition, the binder can be removed suddenly. Also, if the burnout process is performed in the ambient condition even at a lower temperature with a slower heating rate, the binder can be removed too quickly by combustion. Therefore, the change of burnout atmosphere may be an intricate and complex trouble in the fabrication of Ni-MLCCs and the burnout process in the different atmosphere should be adapted through the proper control of the above parameters for the complete binder removal. In addition, the removal rate of the binder will affect the sintering behavior and final microstructural development. Studies related to the effects of processing variables in both burnout and sintering processes on the microstructural development and electrical properties in this system are underway and will be reported later.

4. Conclusions

The effects of the burnout parameters on the binder removal and microstructure have been investigated in $BaTiO_3$ based Ni-MLCCs of X7R characteristic. The ambient condition was more effective in removing the binder than the reducing one. However, the delamination took place at faster heating rate in the ambient condition, showing no defect even at higher temperature (300 °C) and faster heating rate (7 °C) in the reducing one. The temperature and atmosphere in the burnout process was a determining effect on the cumulative pore surface area and burnout microstructure rather than the change of the heating rate, even though the pore size distribution became narrower and the mean pore size larger with an increase of the heating rate. The burnout process should be performed at higher temperature with faster heating rate in the reducing or at lower temperature with slower heating rate in the ambient in this system. Consequently, the atmosphere and temperature in the burnout process play a more important role in preventing the defects and in controlling the microstructure in MLCCs than the heating rate.

Acknowledgements

This work was financially supported by the Korea Institute Science and Technology Evaluation and Planning (KISTEP) through the National Research Laboratory (NRL).

References

[1] Y. Sakabe, Dielectric materials for base-metal multilayer ceramic capacitors, Am. Ceram. Soc. Bull. 66 (1987) 1338–1341.
[2] Y. Mizuno, Y. Okino, N. Kohzu, H. Chazono, H. Kishi, Influence of the microstructure evolution on electrical properties of multilayer capacitors with Ni electrode, Jpn. J. Appl. Phys. 37 (1998) 5227–5231.
[3] Y. Okino, N. Kohzu, Y. Mizuno, M. Honda, H. Chazono, H. Kishi, Effects of the microstructure on dielectric properties for $BaTiO_3$-based MLC with Ni electrode, Key Eng. Mater. 157 (1999) 9–15.
[4] H. Chazono, Y. Okino, N. Kohzu, H. Kishi, Effect of Sm and Ho addition on the microstructure and electrical properties in MLCC with Ni internal electrode, Ceram. Trans. 97 (1999) 53–64.
[5] Y. Mizuno, T. Hagiwara, H. Chazono, H. Kishi, Effect of milling process on core-shell microstructure and electrical properties for BaTiO3-based Ni-MLCC, J. Eur. Ceram. Soc. 21 (2001) 1649–1652.
[6] H. Saito, H. Chazono, H. Kishi, N. Yamaoka, X7R multilayer ceramic capacitor with nickel electrode, Jpn. J. Appl. Phys. 30 (1991) 2307–2310.
[7] I. Burn, Ceramic disk capacitors with base-metal electrodes, Ceram. Bull. 57 (6) (1978) 600–604.
[8] T. Nomura, T. Kato, Y. Nagano, The 9th US–Japan Seminar on Dielectric and Piezoelectric Ceramics, 1999, pp. 295–298.
[9] J. Yamamatsu, N. Kawno, T. Arashi, A. Sato, Y. Nakano, T. Nomura, Reliability of multilayer ceramic capacitors with nickel electrodes, J. Power Sources 60 (1996) 199–203.
[10] D.F.K. Hennings, Dielectric materials for sintering in reducing atmosphere, J. Eur. Ceram. Soc. 21 (2001) 1637–1642.
[11] N. Halder, D. Chattopadhyay, A.D. Sharma, D. Saha, A. Sen, H.S. Maiti, Effect of sintering atmosphere on the dielectric properties of barium titanate based capacitors, Mater. Res. Bull. 36 (1991) 905–913.
[12] Y. Park, Y.H. Kim, H.G. Kim, The effect of grain size on dielectric behavior of $BaTiO_3$ based X7R materials, Mater. Lett. 28 (1996) 101–106.
[13] H.T. Kim, J.H. Adair, M.T. Lanagan, Thermomechanical beha-

vior of BME capacitors during binder burnout, Am. Ceram. Soc. Bull. 80 (10) (2001) 34–38.
[14] N. Das, H.S. Maiti, Formation of pore structure in tape-cast alumina membranes—effects of binder content and firing temperature, J. Membrane Sci. 140 (1998) 205–212.
[15] S. Westermarck, A.M. Juppo, L. Kervinen, J. Yliruusi, Pore structure and surface area of mannitol powder, granules and tablets determined with mercury porosimetry and nitrogen adsorption, Eur. J. Pharm. Biopharm. 46 (1998) 61–68.
[16] L. Moscou, S. Lub, Practical use of mercury porosimetry in the study of porous solids, Powder Tech. 29 (1981) 45–52.
[17] F.A.L. Dullien, Porous media: fluid transport and pore structure, second ed, Academic Press, New York, 1992.
[18] G.P. Matthews, C.J. Ridgway, M.C. Spearing, Void space modeling of mercury intrusion hysteresis in sandstone, paper coating and other porous media, J. Colloid Interface Sci. 171 (1995) 8–27.
[19] S. Lowell, J.E. Shields, Powder surface area and porosity, third ed., Chapman and Hall, New York, 1991.